

## ORIGINAL ARTICLE

Neural transcriptome of constitutional *Pten* dysfunction in mice and its relevance to human idiopathic autism spectrum disorderAK Tilot<sup>1,2,3</sup>, G Bebek<sup>1,2,4</sup>, F Niazi<sup>1,2</sup>, JB Altemus<sup>1,2</sup>, T Romigh<sup>1,2</sup>, TW Frazier<sup>1,2,3,5,6</sup> and C Eng<sup>1,2,3,7,8,9,10</sup>

Autism spectrum disorder (ASD) is a neurodevelopmental condition with a clear, but heterogeneous, genetic component. Germline mutations in the tumor suppressor *Pten* are a well-established risk factor for ASD with macrocephaly, and conditional *Pten* mouse models have impaired social behavior and brain development. Some mutations observed in patients disrupt the normally balanced nuclear-cytoplasmic localization of the *Pten* protein, and we developed the *Pten*<sup>m3m4</sup> model to study the effects of a cytoplasm-predominant *Pten*. In this model, germline mislocalization of *Pten* causes inappropriate social behavior with intact learning and memory, a profile reminiscent of high-functioning ASD. These animals also exhibit histological evidence of neuroinflammation and expansion of glial populations by 6 weeks of age. We hypothesized that the neural transcriptome of this model would be altered in a manner that could inform human idiopathic ASD, a constitutional condition. Using total RNA sequencing, we found progressive disruption of neural gene expression in *Pten*<sup>m3m4</sup> mice from 2–6 weeks of age, involving both immune and synaptic pathways. These alterations include downregulation of many highly coexpressed human ASD-susceptibility genes. Comparison with a human cortical development coexpression network revealed that genes disrupted in *Pten*<sup>m3m4</sup> mice were enriched in the same areas as those of human ASD. Although *Pten*-related ASD is relatively uncommon, our observations suggest that the *Pten*<sup>m3m4</sup> model recapitulates multiple molecular features of human ASD, and that *Pten* operates far upstream of common pathways within ASD pathogenesis.

*Molecular Psychiatry* (2016) **21**, 118–125; doi:10.1038/mp.2015.17; published online 10 March 2015

## INTRODUCTION

Autism spectrum disorder (ASD) is a highly heritable neurodevelopmental condition, characterized by deficits in social communication and restricted, repetitive behaviors.<sup>1,2</sup> Genetic studies of non-syndromic ASD over the last 15 years have identified hundreds of rare genetic variants that may increase susceptibility, many identified only in single reports.<sup>3–7</sup> By contrast, multiple genetic syndromes include high rates of ASD in addition to other phenotypes such as epilepsy (tuberous sclerosis, 40%), motor dysfunction (Rett syndrome, 25–40%) or cancer (*Pten* Hamartoma Tumor syndrome, PHTS, 23%).<sup>8,9</sup> Germline genetic alterations, including rare variants and Mendelian genetic syndromes with high rates of ASD, provide an etiology for ~20% of all cases of ASD.<sup>10</sup> PHTS and other syndromic causes of ASD are powerful avenues for reducing the heterogeneity of the human disorder to focus on its common etiologies. Mouse models based on clinically relevant genetic alterations, with overt symptom overlap, are among the best available mechanisms for realizing this potential.

Several studies indicate that germline *PTEN* mutations occur in up to 10% of children with ASD and macrocephaly. The lifetime risks for multiple cancers in PHTS make genetic testing for *PTEN* mutations crucial within the macrocephalic subgroup of ASD, which represents up to 20% of all ASD cases.<sup>11–13</sup> We recently

described a new mouse model of *Pten* dysfunction based on germline missense mutations that disrupt the intracellular localization of the protein, shifting its normally even distribution toward cytoplasm predominance.<sup>14,15</sup> Germline mutations that shift protein localization have been reported in PHTS patients, such as the nuclear-predominant K62R mutation and the cytoplasm-predominant K289E mutation. Mice homozygous for the *Pten*<sup>m3m4</sup> mutation display social behavior and balance abnormalities without deficits in learning or memory, a profile reminiscent of children with high-functioning ASD. At the cellular level, the mice exhibit increased glial production and significant neuroinflammation by 6-week old.<sup>15</sup>

As the *Pten*<sup>m3m4</sup> mouse shows promising cellular and behavioral phenotypes relevant to idiopathic human ASD as well as those associated with PHTS, our goal was to identify the effects of this mutation on the neural transcriptome. RNA sequencing of the brain at both 2 and 6 weeks of age allowed us to measure the development of genome-wide transcriptional changes in an unbiased fashion with high sensitivity. We hypothesized that germline disruption of this ASD-susceptibility gene could provoke neural gene expression changes reflective of the broader idiopathic ASD transcriptome, suggesting that *PTEN* may operate high up above many signaling pathways relevant to human ASD.

<sup>1</sup>Genomic Medicine Institute, Cleveland Clinic, Cleveland, OH, USA; <sup>2</sup>Lerner Research Institute, Cleveland Clinic, Cleveland, OH, USA; <sup>3</sup>Department of Molecular Medicine, Case Western Reserve University School of Medicine, Cleveland, OH, USA; <sup>4</sup>Center for Proteomics and Bioinformatics, Case Western Reserve University School of Medicine, Cleveland, OH, USA; <sup>5</sup>Center for Autism, Pediatric Institute, Cleveland Clinic, Cleveland, OH, USA; <sup>6</sup>Department of Pediatrics, Case Western Reserve University School of Medicine, Cleveland, OH, USA; <sup>7</sup>Taussig Cancer Institute, Cleveland Clinic, Cleveland, OH, USA; <sup>8</sup>Stanley Shalom Zielony Institute of Nursing Excellence, Cleveland Clinic, Cleveland, OH, USA; <sup>9</sup>Department of Genetics and Genome Sciences, Case Western Reserve University School of Medicine, Cleveland, OH, USA and <sup>10</sup>CASE Comprehensive Cancer Center, Case Western Reserve University School of Medicine, Cleveland, OH, USA. Correspondence: Professor C Eng, Genomic Medicine Institute, Cleveland Clinic, 9500 Euclid Avenue, Mailstop NE-50, Cleveland, OH 44195, USA.

E-mail: engc@ccf.org

Received 23 September 2014; revised 12 December 2014; accepted 8 January 2015; published online 10 March 2015

## MATERIALS AND METHODS

### Animals and experimental design

The *Pten*<sup>m3m4</sup> model is based on germline mutations to the 3rd and 4th localization sequences of the mouse *Pten* gene. *Pten* protein mislocalization and expression were previously confirmed in brain tissue lysates and cultured neurospheres.<sup>15</sup> Male wild-type (Wt), *Pten*<sup>wt/m3m4</sup> and *Pten*<sup>m3m4/m3m4</sup> mice on the CD-1 genetic background were generated via heterozygous crossings and aged until 2 or 6-week old. The 2-week-old cohort was taken from a single litter, whereas the 6-week-old cohort represented two separate litters. Three animals per genotype and age were used as biological replicates, as we estimated that this would provide reasonable power to detect large expression changes when combined with sequencing of ~66 million reads per sample (Supplementary Table 1). We found that at  $n = 3$  and 0.1 coefficient of variance (determined using R package CummeRbund), we could detect fold differences of 1.97 at a power of 0.8 (Bioconductor package RNASeqPower). No randomization was used to select animals for each group, and investigators were not blinded to genotype. Animals were killed by CO<sub>2</sub> asphyxiation followed by cervical dislocation (2-week cohort), or exsanguination with phosphate-buffered saline (6-week cohort). Single hemispheres (2 weeks) and microdissected cortices (6 weeks) were flash frozen immediately following killing. All procedures carried out were approved by the Cleveland Clinic Institutional Animal Care and Use Committee. The RNA-sequencing data is available through the NCBI Gene Expression Omnibus, using accession number GSE59318.

### Tissue preparation and RNA isolation

Flash-frozen tissues were homogenized in 1 ml Trizol (Life Technologies, Carlsbad, CA, USA) using 5 mm stainless-steel beads for 2 minutes at 25 Hz with a TissueLyserII (Qiagen, Valencia, CA, USA). Total RNA was isolated using Trizol according to the manufacturer's protocol. Ambion PureLink RNA Mini Kit (Life Technologies) was utilized for RNA clean-up and DNase. In short, 15 µg total RNA mixed with lysis buffer:ethanol (1:3) was applied to the column and rinsed with Wash Buffer II (70% ethanol). DNA was digested on column for 15 min with PureLink DNase (Life Technologies) and RNA was rinsed twice with Wash Buffer II (70% ethanol). RNA quality was assessed via Bioanalyzer, and 5 µg DNase-RNA was shipped to Genome Quebec for library prep and sequencing.

### Library preparation and RNA sequencing

Sequencing libraries were prepared using the Illumina TruSeq Stranded Total RNA with Ribo Zero kit (Illumina, San Diego, CA, USA). The libraries were multiplexed three to a lane, grouped in biological triplicates. Hundred base pair, paired-end sequencing was performed using the Illumina HiSeq platform.

### Read mapping and quantification of gene expression

Sequencing reads were aligned to the mouse mm10 reference genome using Tophat (versions 2.0.8–2.0.11)/Bowtie (versions 2.0.2–2.2.0) and assembled into RNA transcripts using the Cufflinks package (versions 2.0.2–2.2.0).<sup>16,17</sup> Following calculation of FPKM values (fragments per kilobase of exon model per million mapped fragments), we calculated differential expression using Cuffdiff 2 (versions 2.0.2–2.2.0). Following predetermined contrasts, we calculated differential expression by comparing Wt FPKM values to those of *Pten*<sup>wt/m3m4</sup> or *Pten*<sup>m3m4/m3m4</sup> mice individually for each age. Transcripts were considered differentially expressed at  $q < 0.05$  following Benjamini–Hochberg multiple testing correction of the original *P*-values.<sup>16</sup> Multidimensional scaling was performed using the R-project package cummeRbund (version 2.4.1), whereas the correlation between differential expression levels at 2 and 6 weeks of age was calculated using the R-project package stats (version 3.0.2).

### Pathway analysis and comparison with AutDB

Differentially expressed genes within each comparison group were analyzed using Ingenuity Pathway Analysis (Ingenuity Systems, Redwood City, CA, USA, www.ingenuity.com). AutDB is a manually curated public database of genes associated with ASD (http://autism.mindspec.org/autdb/HG\_Home.do, accessed 20 June 2014).<sup>18</sup> We used all genes listed in the database for comparison with differentially expressed genes in the *Pten*<sup>m3m4</sup> mouse by two-tailed Fisher's exact test using the R-project package stats (version 3.0.2). The minimal distance network was based on

the set of 69 genes within AutDB that were differentially expressed in at least one comparison group. Additional nodes (smaller font size) were introduced if they directly linked two AutDB genes (larger font size), and the network was generated using the R-project package igraph (version 0.7.1). Incorporation of differential expression data from the 6-week-old Wt vs *Pten*<sup>m3m4/m3m4</sup> comparison, and gene ontology analysis was performed using Cytoscape (version 3.3.1), and the plugin BiNGO (version 3.0.2).

### Comparison with coexpression network from Parikshak *et al.*

The expression modules identified by Parikshak *et al.* were based on analysis of RNAseq data from the Brainspan database of human neural gene expression from ages post conception week 8 through 1 year, using weighted gene coexpression network analysis.<sup>19–21</sup> *Pten*<sup>m3m4</sup> differentially expressed genes were first converted to their corresponding human orthologs using BioMart (accessed 4 March 2014).<sup>22</sup> Genes associated with each module were accessed via the original article's supplementary information, available online (http://www.cell.com/cell/abstract/S0092-8674(13)01349-4, accessed 23 March 14), and compared with the differentially expressed genes identified in *Pten*<sup>m3m4</sup> mice using two-tailed Fisher's exact test (R-project package stats, version 3.0.2).

## RESULTS

### RNA sequencing reveals progressive alteration in gene expression in *Pten*<sup>m3m4</sup> mice

We utilized RNA sequencing to study the neural transcriptome of *Pten*<sup>m3m4</sup> mice across their development in an unbiased fashion. Total RNA was isolated from hemibrains at age 2 weeks, and from microdissected cortex at age 6 weeks—when this model demonstrates both social and neuroinflammatory phenotypes.<sup>15</sup> In mice, these ages represent an early juvenile stage and adolescence, respectively, periods in human development when ASD symptoms can be readily identified. At both ages, we compared samples from Wt mice with those from heterozygous (*Pten*<sup>wt/m3m4</sup>) and homozygous (*Pten*<sup>m3m4/m3m4</sup>) mice, using three biological replicates in each group (Figure 1a).

RNA sequencing generated an average of 66 million paired-end reads per sample, an average of 89% mapping to the mouse mm10 genome (Supplementary Table 1). *Pten* was not differentially expressed in any of the comparison groups, as appropriate (Figure 1b).<sup>15</sup> Using multidimensional scaling to reduce the variation between sample groups to a single point in two-dimensional space, Wt and *Pten*<sup>wt/m3m4</sup> samples clustered tightly together within an age, but separated greatly between ages (Figure 1d). By contrast, the *Pten*<sup>m3m4/m3m4</sup> samples separated from the Wt and *Pten*<sup>wt/m3m4</sup> samples at both ages. These genotypic and age differences seen were reflected in the total numbers of differentially expressed genes (false-discovery rate corrected *P*-value of  $< 0.05$ ). By 2 weeks of age, there were 364 differentially expressed genes in the *Pten*<sup>m3m4/m3m4</sup> brain compared with Wt (48 downregulated), and 181 for *Pten*<sup>wt/m3m4</sup> samples (53 downregulated). Compared with Wt mice at 6 weeks of age, there were 1377 differentially expressed genes in the *Pten*<sup>m3m4/m3m4</sup> cortex (484 downregulated) and only 75 for *Pten*<sup>wt/m3m4</sup> mice (28 downregulated). This is consistent with the much smaller extent of cellular and behavioral phenotypes seen in the *Pten*<sup>wt/m3m4</sup> animals.<sup>15</sup>

Three genes were differentially expressed across both genotypes at both ages, *Fcrls* (Fc receptor-like 5, scavenger receptor), *Agxt2l1* (ethanolamine phosphate phospholyase) and *Egr2* (early growth response 2), although there were 152 genes differentially expressed in both the 2-week and 6-week *Pten*<sup>m3m4/m3m4</sup> samples compared with wild type (Figure 1c). Within genes that were differentially expressed at both ages, the fold-changes in expression at each age were positively correlated for both genotypes, but only statistically significant in *Pten*<sup>m3m4/m3m4</sup> mice owing to reduced overlap between ages for *Pten*<sup>wt/m3m4</sup> (Pearson's, *Pten*<sup>wt/m3m4</sup>  $r = 0.67$ ,  $P$ -value = 0.21, *Pten*<sup>m3m4/m3m4</sup>  $r = 0.74$ ,  $P$ -value =  $2.2 \times 10^{-16}$ , Figure 1e).

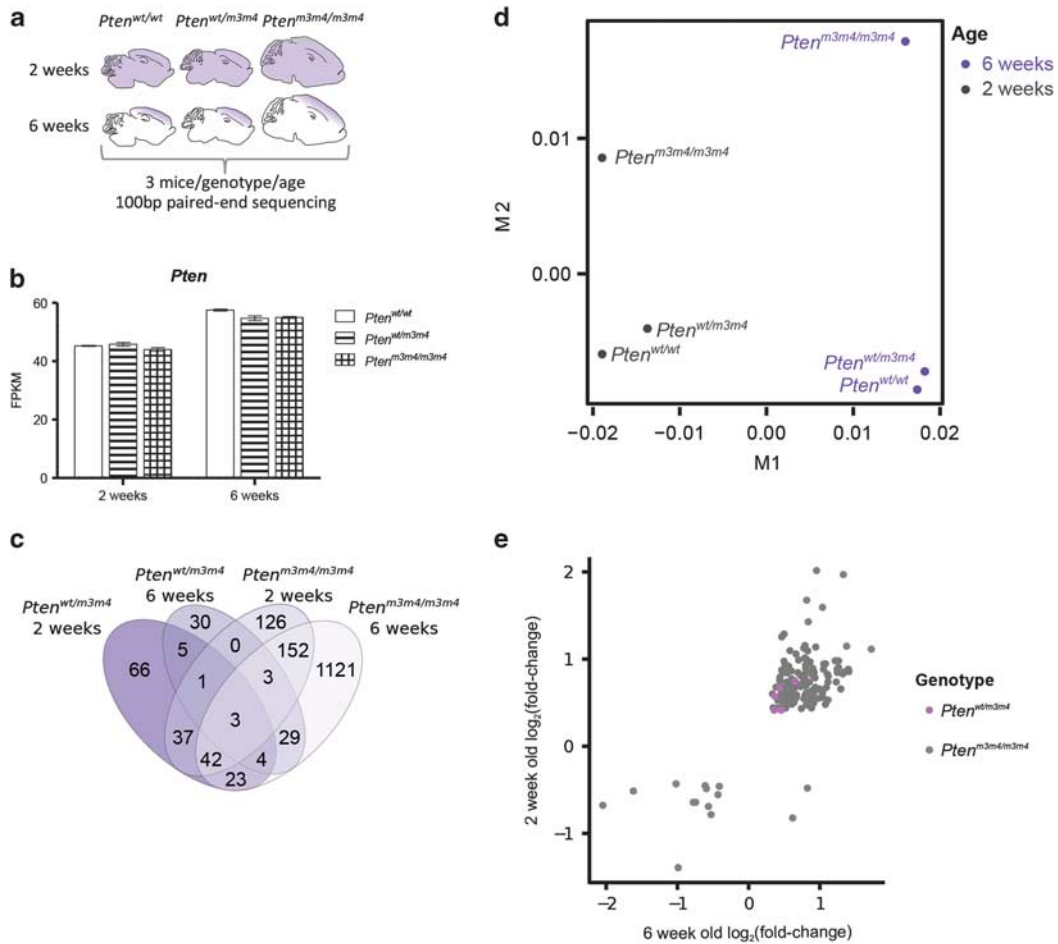


**Figure 1.** The *Pten*<sup>m3m4</sup> mutation causes progressive and dose-dependent changes in neural gene expression. **(a)** Schematic of the experimental design. Drawings represent the differences in general size and shape of the brain between genotypes, whereas purple shading indicates the brain area used for RNA isolation. **(b)** *Pten* expression levels are unchanged from wild-type across genotypes and ages (*t*-tests, FDR corrected *P*-value >0.05, *n* = 3 biological replicates per genotype and age). Error bars represent one standard error of the mean (s.e.m.). **(c)** Venn diagram illustrating the extent of overlap among the differentially expressed genes observed in each genotype at each age. **(d)** Multidimensional scaling shows separation of samples by age (M1), then by genotype (M2). **(e)** For genes that are differentially expressed at both 2 and 6 weeks, the log<sub>2</sub> (fold-change) in gene expression is correlated between ages (Pearson).

#### Increasing alteration of ASD-linked pathways with age and dose of mutant Pten

We next questioned what biological functions were most associated with these differences in gene expression, and whether such disruptions became more apparent with time. As the *Pten*<sup>m3m4/m3m4</sup> animals display the greatest alterations in gene expression, we focused on differentially expressed genes in this genotype compared with Wt animals of the same age. We used Ingenuity Pathway Analysis to determine the top canonical pathways implicated by genes that were either upregulated (Figure 2, purple bars) or downregulated (Figure 2, green bars) at 2 and 6 weeks. Within upregulated pathways, the significance of the overall pathway involvement increased between 2 and 6 weeks of age.

Several of the most upregulated canonical pathways involved inflammatory or immune processes such as IL-8 and NF-κB signaling, leukocyte extravasation and dendritic cell maturation (Figure 2).<sup>15</sup> The downregulated genes in *Pten*<sup>m3m4/m3m4</sup> cortex fell largely into pathways relating to synaptic activity (Figure 2).<sup>20</sup> Specifically, both glutamate and serotonin receptor signaling pathways were downregulated, as well as calcium signaling and a multitude of G-protein coupled receptor pathways.

#### Many ASD-susceptibility genes are downregulated in the *Pten*<sup>m3m4</sup> cortex

We compared the differentially expressed genes from each of the four comparison groups with ASD-susceptibility genes reported in AutDB, a manually curated database of > 500 genes considered associated with ASD via genetic or functional studies.<sup>18</sup> There was significant enrichment of AutDB genes within the differentially expressed genes of the *Pten*<sup>m3m4/m3m4</sup> cortex (Fisher's exact test, odds ratio = 1.59, *P*-value = 0.0013), with 62 ASD-related genes differentially expressed (Table 1 and Supplementary Table 2). AutDB genes were not enriched within the differentially expressed genes of the *Pten*<sup>wt/m3m4</sup> samples or the 2-week-old *Pten*<sup>m3m4/m3m4</sup> samples. Despite this, the overlapping ASD-susceptibility genes identified in patients through deletions or nonsense mutations were largely downregulated in the *Pten*<sup>m3m4/m3m4</sup> cortex (69%, Table 1). One additional gene, *SLC16A3*, was upregulated in *Pten*<sup>m3m4/m3m4</sup> mice, although both deletions and duplications are reported in the ASD literature.<sup>7</sup>

To determine whether these genes represent a unique signature of ASD or a broader neurodevelopmental or neuroinflammatory signal, we looked for enrichment of the differentially expressed genes seen in our homozygous *Pten*<sup>m3m4</sup> 6-week-old



**Figure 2.** By 6 weeks of age, canonical pathway alterations in *Pten*<sup>m3m4/m3m4</sup> cortex reflect those seen in transcriptome studies of human ASD. Canonical pathway analysis was performed using Ingenuity Pathway Analysis, the top 20 pathways implicated by upregulated genes are shown in purple (top), and those implicated by downregulated genes are shown in green (bottom). The axes indicate the significance of the pathway involvement, and lighter colored inset bars represent the pathway's significance in the 2-week-old samples.

**Table 1.** Many genes reported as deleted in human ASD are downregulated in *Pten*<sup>m3m4/m3m4</sup> mice at 6 weeks of age

AutDB description			<i>Pten</i> <sup>m3m4</sup> expression	
Gene	Alteration in ASD	Variant categories observed	Log <sub>2</sub> (FC)	q-value
<i>CELF6</i>	Genetic association/rare single gene variant/functional	Deletions	-0.465	0.025
<i>GALNT13</i>	Rare single gene variant		-0.429	0.004
<i>ARHGAP15</i>	Rare single gene variant	Deletions, other	-0.529	0.003
<i>CHRN3</i>	Rare single gene variant		-0.962	0.046
<i>NELL1</i>	Genetic association		-0.386	0.008
<i>PCDH15</i>	Genetic association		0.637	0.001
<i>ADCY5</i>	Rare single gene variant	Deletions, missense mutations	-0.365	0.016
<i>AGMO</i>	Genetic association		0.501	0.042
<i>DOCK10</i>	Rare single gene variant		0.529	0.001
<i>PTCHD1</i>	Rare single gene variant		-0.350	0.049
<i>SYN2</i>	Genetic association		0.401	0.016
<i>CADPS2</i>	Rare single gene variant	Deletions, missense mutations, other	-0.325	0.049
<i>GPR37</i>	Rare single gene variant		0.524	0.001
<i>GRIK2</i>	Genetic association		-0.531	0.001
<i>IL1RAPL1</i>	Rare single gene variant		-0.402	0.012
<i>KANK1</i>	Rare single gene variant		0.586	0.001
<i>AHI1</i>	Rare single gene variant	Deletions, duplications, missense mutations, other	-0.648	0.001
<i>CHD2</i>	Multigenic CNV		-0.374	0.039
<i>CNTN5</i>	Rare single gene variant		-0.533	0.001
<i>CNTNAP2</i>	Syndromic		-0.341	0.037
<i>CREBBP</i>	Syndromic		-0.324	0.050
<i>CTTNBP2</i>	Rare single gene variant		-0.405	0.005
<i>DCX</i>	Rare single gene variant		-0.590	0.001
<i>DHCR7</i>	Syndromic		0.818	0.001
<i>DMD</i>	Genetic association		-0.372	0.011
<i>FOXP1</i>	Rare single gene variant		-0.410	0.031
<i>FOXP2</i>	Rare single gene variant		-0.391	0.007
<i>FOXP2</i>	Rare single gene variant		-1.019	0.001
<i>HEPACAM</i>	Rare single gene variant		0.433	0.006
<i>LAMC3</i>	Rare single gene variant		0.600	0.007
<i>RELN</i>	Genetic association		-0.414	0.007
<i>SLC16A3</i>	Rare single gene variant		0.912	0.006

Abbreviations: ASD, autism spectrum disorder; FC, fold change; CNV, copy number variant. See Supplementary Table 2 for the full list of altered susceptibility genes, their primary references and differential expression information for the 2-week-old cohort.

samples within several databases of genes linked to other neurological disorders. After comparison with AlzGene (Alzheimer's disease), MSGene (multiple sclerosis), SZGene (schizophrenia) and ADHDGene (attention deficit hyperactivity disorder), we found a significant enrichment for all but the MSGene list. Assessing the overlap between the *Pten*<sup>m3m4</sup> genes found within each list, more than half of the AutDB genes (34/62) were unique. To determine whether these candidate gene lists had a high degree of overlap, we compared each of the other neurological disorder databases with AutDB. Enrichment of AutDB genes within these other neurological databases was very high (Supplementary Table 3), consistent with reports showing overlap in candidate genes between Alzheimer's and multiple sclerosis, as well as ASD and schizophrenia.<sup>23,24</sup>

Six of the 62 ASD-genes were differentially expressed at both 2 and 6 weeks of age. Among those was *Foxp2*, a transcription factor considered important in the evolution of language and speech.<sup>25</sup> In *Pten*<sup>m3m4</sup> mice, *Foxp2* was downregulated at both ages, with effect size becoming greater with age (Figure 3a). In addition, we found significant upregulation of *Msn*, a gene targeted by a non-coding RNA overexpressed in ASD. In contrast to the typical silencing effect of non-coding RNAs, this targeting leads to upregulation of the *MSN* gene in cell lines, indicating that the upregulation of *Msn* in *Pten*<sup>m3m4/m3m4</sup> mice is directionally appropriate (Figure 3b).<sup>26</sup> Expanding this list to include all AutDB genes differentially expressed in at least one comparison group, we generated a minimal distance interaction network that was

densely connected (Figure 3c). Gene ontology analysis of the entire network revealed enrichment of network genes within the ontologies synaptic transmission (GO: 0007268, circles outlined in orange) and immune system process (GO: 0002376, circles outlined in light blue). Validation that decreased gene expression measured via RNAseq corresponds to decreased protein levels is presented for *Foxp2* and *Cntnap2* in Supplementary Figure 1.

Differentially expressed genes in *Pten*<sup>m3m4</sup> cortex are enriched in gene expression modules of the neurotypical developing human brain corresponding to immune and ASD-related functions

To determine the parallels between gene expression changes in the *Pten*<sup>m3m4</sup> brain with those of human ASD, we needed to examine the murine alterations in the context of normal human brain development. To accomplish this, we utilized the weighted gene coexpression network of human brain development published by Parikshak et al. (Materials and Methods).<sup>21</sup> We first identified the human orthologs of the mouse differentially expressed genes for each age and genotype using BioMart.<sup>22</sup> Next, we looked for enrichment of those genes within each expression module in the human brain coexpression network. Differentially expressed genes from *Pten*<sup>m3m4/m3m4</sup> mice at both 2 and 6 weeks of age were significantly enriched in module M13, which was previously found to be enriched for both ASD-susceptibility genes and genes differentially expressed in ASD cortical samples (Figure 4).<sup>21</sup> Two human cortex gene expression modules related

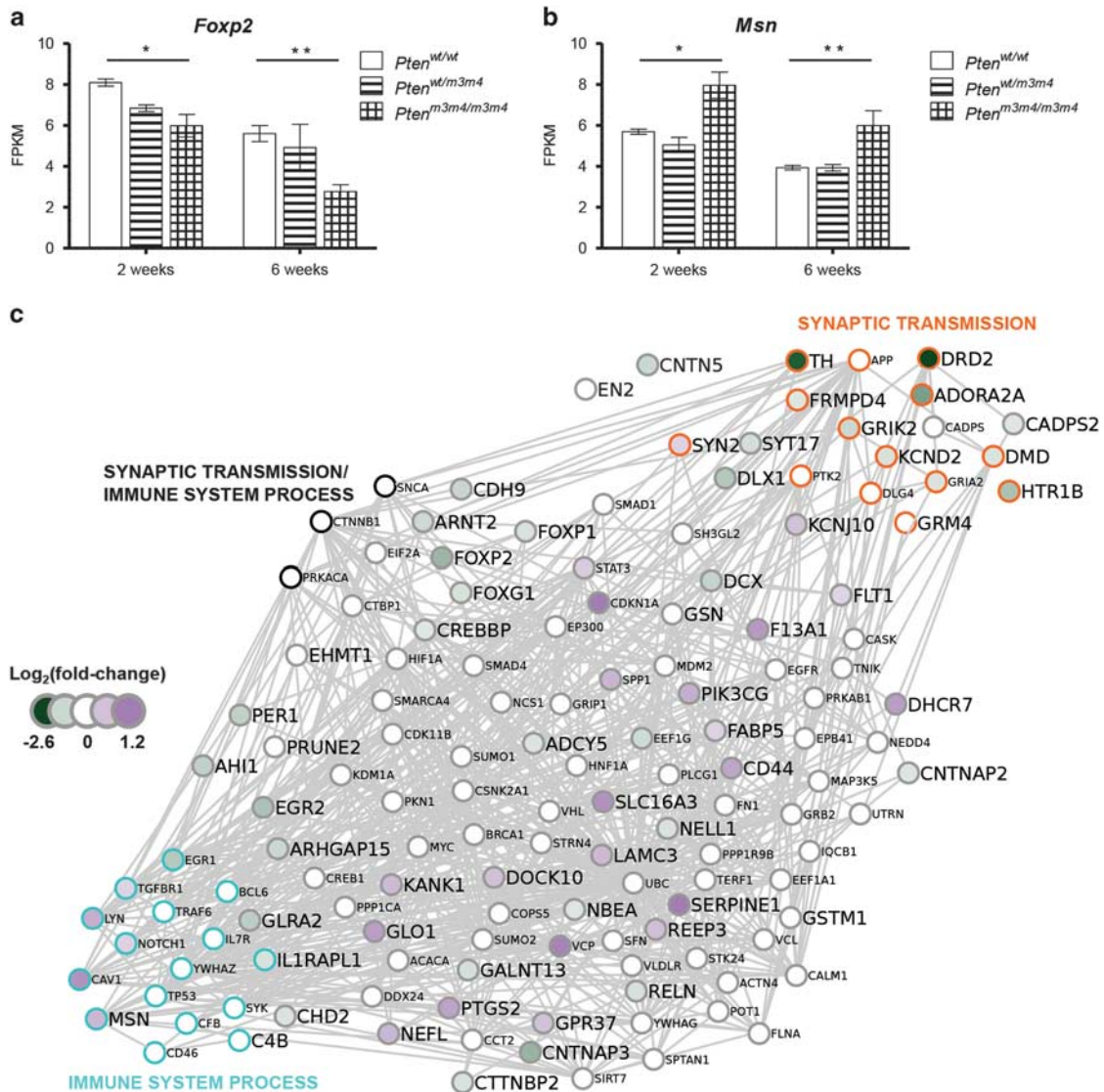


**Figure 3.** Multiple ASD-susceptibility genes are differentially expressed at both 2 and 6 weeks of age, in the direction suggested by the type of variant (*t*-tests,  $n=3$  biological replicates per genotype and age, \*indicates FDR corrected  $P$ -value  $< 0.05$ , \*\*indicates  $P < 0.01$ , error bars represent s.e.m.). **(a)** *Foxp2* is downregulated in *Pten*<sup>*m3m4/m3m4*</sup> mice, and deletions of the human gene are reported in ASD. **(b)** *Msn* levels are increased, and functional validation of a ncRNA upregulated in ASD indicates that its targeting of the human *MSN* gene leads to upregulation. **(c)** Minimal distance interaction network representing all AutDB genes differentially expressed in at least one comparison group (larger font size). Interaction partners that connect two AutDB genes are shown in small font sizes, and the log<sub>2</sub> (fold-change) between wild-type and *Pten*<sup>*m3m4/m3m4*</sup> mice at 6 weeks is shown as node fill colors ranging from purple (upregulated) to green (downregulated). Membership in the gene ontology categories synaptic transmission and immune system process are indicated with node outline colors of orange and light blue, respectively.

to immune system activity, M15 and M18, were also enriched in both *Pten*<sup>*m3m4/m3m4*</sup> and *Pten*<sup>*wt/m3m4*</sup> samples at both 2 and 6 weeks of age. The differentially expressed genes in heterozygous mice were enriched in M13 at 2, but not 6 weeks.

## DISCUSSION

In this study, we utilized RNA sequencing to identify the major pathogenic processes in a mouse model based on alteration of an ASD-susceptibility gene that regulates a host of cellular processes. Consistent with our previous finding that cellular and behavioral phenotypes were largely restricted to the *Pten*<sup>*m3m4/m3m4*</sup> animals, this genotype displayed  $> 10$  times the number of differentially expressed genes seen in *Pten*<sup>*wt/m3m4*</sup> mice.<sup>15</sup> Two themes stood out among the altered genes, namely, increased expression of immune

pathways and decreased expression of synaptic pathways. That the *Pten*<sup>*m3m4*</sup> mutation disrupted functional areas consistently altered in studies of idiopathic ASD, including the downregulation of many ASD-susceptibility genes, is at first surprising, but suggests that PTEN-related pathways may have a major role in ASD pathogenesis. This hypothesis, and potential of *Pten* disruption as a model for idiopathic ASD, is supported by its regulation of synaptic plasticity, neuronal migration and dendritic arborization via the PI3K/AKT/mTOR pathway and other, less understood, mechanisms.<sup>27–29</sup>

In 6-week-old *Pten*<sup>*m3m4/m3m4*</sup> animals, many of the gene expression changes were linked to immune system activation. That this process was detectable in the 2-week-old *Pten*<sup>*m3m4*</sup> brain (Figures 2 and 4) extends our earlier findings of reactive astrogliosis and microglial activation in the *Pten*<sup>*m3m4/m3m4*</sup> brain at 6 weeks.<sup>15</sup> Although the results confirmed immune system

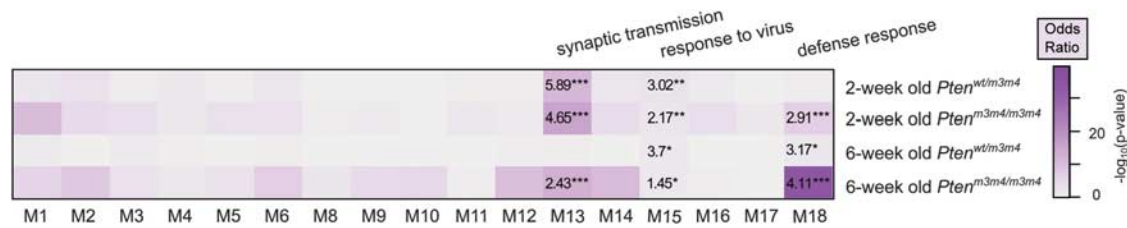


**Figure 4.** Differentially expressed genes in *Pten*<sup>m3m4</sup> mice are enriched in gene expression modules of the developing human brain that represent immune responses and synaptic transmission. The heatmap represents the  $-\log_{10}(P\text{-value})$  of the two-tailed Fisher's exact test for enrichment of differentially expressed genes within each individual module of the weighted gene coexpression network published by Parikhshak *et al.*<sup>21</sup> Numbers within a cell correspond to the Fisher's test odds ratio. Gene ontology terms most enriched in the significant modules are listed above. \*indicates  $P$ -values  $< 0.05$ , \*\*  $< 0.01$  and \*\*\*  $< 0.001$ .

activation in the model, they did not point to a specific initial stimulus. Rather, the data suggested upregulation of immune processes that were either nonspecific (for example, interleukin-1 and nuclear factor- $\kappa$ B responses), or pointed toward multiple potential starting points (for example, upregulation of both TLR1 and TLR3). Histological studies of post mortem ASD brains found similar evidence for neuroinflammation in patients as young as 3 years of age.<sup>30,31</sup> More recent transcriptome studies support the histological reports, demonstrating increased expression of immune system-related genes across multiple reports and methodologies.<sup>20,32</sup>

The downregulation of multiple pathways related to the normal function of synapses in the *Pten*<sup>m3m4</sup> model provokes several questions (Figure 2). These effects occur despite normal neuron number and minimal effects of the *Pten*<sup>m3m4</sup> mutation on neuronal morphology, suggesting causative mechanisms beyond PI3K/mTOR-induced hypertrophy.<sup>15</sup> This hypothesis is supported by a report showing that cellular hypertrophy was unconnected to synaptic changes in a mouse model of neuron-specific *Pten* loss.<sup>27</sup> We speculate that many of these downregulation events are an indirect effect of *Pten* disruption, occurring downstream of increased expression of transcription factors or activation of pathways normally inhibited by *Pten* activity. Overproduction of astrocytes in the *Pten*<sup>m3m4</sup> brain should not be overlooked as a potential driver of synaptic dysfunction, a major area of ASD research.<sup>15,33–35</sup> Functional magnetic resonance imaging studies report decreased functional connectivity across multiple regions of the ASD brain, and decreased expression of synaptic genes was a major finding in the ASD cortical transcriptome.<sup>20,36,37</sup> As that same study reported disruption of glial gene expression signatures, how changes to glial activity in response to inflammatory stimuli affect their regulation of synapses is an open question.<sup>20</sup>

The decreased expression of  $>60$  ASD-susceptibility genes in the *Pten*<sup>m3m4/m3m4</sup> cortex by 6 weeks of age indicates that the normal activity of these genes is regulated by *Pten*-related pathways (Table 1 and Figure 3). Enrichment of *Pten*<sup>m3m4/m3m4</sup> differentially expressed genes within the susceptibility genes of other neurological disorders may point to a common set of gene expression differences that occur in cases of neuroinflammation (Alzheimer's/MS) or synaptic dysfunction (ASD/Schizophrenia). Most of the *Pten*<sup>m3m4/m3m4</sup> differentially expressed genes found in AutDB were unique to ASD, and may represent a distinct set of ASD-linked processes disrupted in these animals. That these susceptibility genes were also enriched in gene ontologies relating to synaptic and immune functions underscores the importance of these pathways from the genetics to histopathology of ASD (Figure 3).

Weighted gene coexpression network analysis is a powerful tool for uncovering how clusters of genes relate to each other (for example, trajectory of expression during development) and to specific phenotypes (for example, ASD or intellectual disability). Utilizing this tool to explore how the gene expression differences we observed in *Pten*<sup>m3m4</sup> mice relate to human cortical

development, we found striking parallels to idiopathic ASD. The *Pten*<sup>m3m4</sup> alterations mapped to the expression network of the neurotypical human brain in some of the same ways as alterations observed

in ASD at both the transcriptional and susceptibility gene levels (Figure 4).<sup>21</sup> That these points of divergence from normal development related to synaptic transmission and immune responses supports our conclusion that the *Pten*<sup>m3m4</sup> mutation alters multiple neural cell types in ways functionally important to the pathogenesis of ASD.

There are limitations to the current study that should be noted. The *Pten*<sup>m3m4</sup> mutation produces diminished levels of a mis-localized protein, potentially better tolerated by mice than humans. Such differences may underlie the subtle phenotype of heterozygous *Pten*<sup>m3m4</sup> mice, and represent a common limitation of mouse models of human disease. Our ability to detect differences in the 2-week samples was likely reduced by the increased heterogeneity of whole brain tissue compared with microdissected cortex. It is possible that ASD-susceptibility genes or those related broadly to synaptic activity are significantly disrupted at this earlier stage. Larger sample sizes would have aided detection of such differences. Despite these limitations, the presence of so many ASD-susceptibility genes within the altered landscape of the *Pten*<sup>m3m4</sup> transcriptome suggest that the model exhibits fundamental similarities to human ASD arising from both syndromic (PHTS) and non-syndromic (idiopathic, rare variant) causes.

This study places PTEN far upstream in the pathogenesis of ASD, as germline alterations to its function produced transcriptional changes impacting central aspects of the disorder. With recent advances in our understanding of the ASD transcriptome, we can now focus on animal model-based studies on the mechanisms behind the behavioral phenotypes and their amenability to treatment and in time, prevention. The greatest benefit will come from those models where ASD-like behaviors arise from the dysfunction of the same pathways that are altered in human ASD.<sup>38</sup> A logical next step for these studies will be functional analyses guided by the synaptic dysfunction suggested by our data. In addition, investigation of embryonic and early postnatal time points for evidence of neuroinflammation is warranted, as its presence can be appreciated by as early as 2 weeks, before synaptic dysfunction manifests as disrupted signaling networks (Figure 2).

#### CONFLICT OF INTEREST

The authors declare no conflict of interest.

#### ACKNOWLEDGMENTS

We are grateful to Dr Robert Miller and Dr Jonathan Smith for their critical assessment of the findings. This work was supported, in part, by the National Institutes of Health (R01CA118989 to CE), and a generous gift from Sam H Miller. CE is the Sondra J and

Stephen R Hardis Endowed Chair of Cancer Genomic Medicine at the Cleveland Clinic, and is an ACS Clinical Research Professor.

## REFERENCES

- Freitag CM. The genetics of autistic disorders and its clinical relevance: a review of the literature. *Mol Psychiatry* 2007; **12**: 2–22.
- Frazier TW, Youngstrom EA, Speer L, Embacher R, Law P, Constantino J *et al*. Validation of proposed DSM-5 criteria for autism spectrum disorder. *J Am Acad Child Adolesc Psychiatry* 2012; **51**: 28–40 e23.
- O’Roak BJ, Vives L, Girirajan S, Karakoc E, Krumm N, Coe BP *et al*. Sporadic autism exomes reveal a highly interconnected protein network of *de novo* mutations. *Nature* 2012; **485**: 246–250.
- Michaelson JJ, Shi Y, Gujral M, Zheng H, Malhotra D, Jin X *et al*. Whole-genome sequencing in autism identifies hot spots for *de novo* germline mutation. *Cell* 2012; **151**: 1431–1442.
- Ben-David E, Shifman S. Combined analysis of exome sequencing points toward a major role for transcription regulation during brain development in autism. *Mol psychiatry* 2013; **18**: 1054–1056.
- Schaaf CP, Sabo A, Sakai Y, Crosby J, Muzny D, Hawes A *et al*. Oligogenic heterozygosity in individuals with high-functioning autism spectrum disorders. *Hum Mol Genet* 2011; **20**: 3366–3375.
- Pinto D, Pagnamenta AT, Klei L, Anney R, Merico D, Regan R *et al*. Functional impact of global rare copy number variation in autism spectrum disorders. *Nature* 2010; **466**: 368–372.
- Mount RH, Charman T, Hastings RP, Reilly S, Cass H. Features of autism in Rett syndrome and severe mental retardation. *J Autism Dev Disord* 2003; **33**: 435–442.
- Sandberg AD, Ehlers S, Hagberg B, Gillberg C. The Rett syndrome complex: communicative functions in relation to developmental level and autistic features. *Autism* 2000; **4**: 249–267.
- Jeste SS, Geschwind DH. Disentangling the heterogeneity of autism spectrum disorder through genetic findings. *Nat Rev Neurol* 2014; **10**: 74–81.
- Butler MG, Dasouki MJ, Zhou XP, Talebizadeh Z, Brown M, Takahashi TN *et al*. Subset of individuals with autism spectrum disorders and extreme macrocephaly associated with germline PTEN tumour suppressor gene mutations. *J Med Genet* 2005; **42**: 318–321.
- McBride KL, Varga EA, Pastore MT, Prior TW, Manickam K, Atkin JF *et al*. Confirmation study of PTEN mutations among individuals with autism or developmental delays/mental retardation and macrocephaly. *Autism Res* 2010; **3**: 137–141.
- Tan MH, Mester J, Peterson C, Yang Y, Chen JL, Rybicki LA *et al*. A clinical scoring system for selection of patients for PTEN mutation testing is proposed on the basis of a prospective study of 3042 probands. *Am J Hum Genet* 2011; **88**: 42–56.
- Mester JL, Tilot AK, Rybicki LA, Frazier TW 2nd, Eng C. Analysis of prevalence and degree of macrocephaly in patients with germline PTEN mutations and of brain weight in Pten knock-in murine model. *Eur J Hum Genet* 2011; **19**: 763–768.
- Tilot AK, Gaugler MK, Yu Q, Romigh T, Yu W, Miller RH *et al*. Germline disruption of Pten localization causes enhanced sex-dependent social motivation and increased glial production. *Hum Mol Genet* 2014; **23**: 3212–3227.
- Trapnell C, Hendrickson DG, Sauvageau M, Goff L, Rinn JL, Pachter L. Differential analysis of gene regulation at transcript resolution with RNA-seq. *Nat Biotechnol* 2013; **31**: 46–53.
- Trapnell C, Roberts A, Goff L, Pertea G, Kim D, Kelley DR *et al*. Differential gene and transcript expression analysis of RNA-seq experiments with TopHat and Cufflinks. *Nat Protoc* 2012; **7**: 562–578.
- Basu SN, Kollu R, Banerjee-Basu S. AutDB: a gene reference resource for autism research. *Nucleic Acids Res* 2009; **37**(Database issue): D832–D836.
- Zhang B, Horvath S. A general framework for weighted gene co-expression network analysis. *Stat Appl Gene Mol Biol* 2005; **4**, Article17.
- Voineagu I, Wang X, Johnston P, Lowe JK, Tian Y, Horvath S *et al*. Transcriptomic analysis of autistic brain reveals convergent molecular pathology. *Nature* 2011; **474**: 380–384.
- Parikshak NN, Luo R, Zhang A, Won H, Lowe JK, Chandran V *et al*. Integrative functional genomic analyses implicate specific molecular pathways and circuits in autism. *Cell* 2013; **155**: 1008–1021.
- Kasprzyk A. BioMart: driving a paradigm change in biological data management. *Database* 2011; **2011**: bar049.
- Crespi B, Stead P, Elliot M. Evolution in health and medicine Sackler colloquium: Comparative genomics of autism and schizophrenia. *Proc Natl Acad Sci USA* 2010; **107**(Suppl 1): 1736–1741.
- Lambert JC, Ibrahim-Verbaas CA, Harold D, Naj AC, Sims R, Bellenguez C *et al*. Meta-analysis of 74,046 individuals identifies 11 new susceptibility loci for Alzheimer’s disease. *Nat Genet* 2013; **45**: 1452–1458.
- Graham SA, Fisher SE. Decoding the genetics of speech and language. *Curr Opin Neurobiol* 2013; **23**: 43–51.
- Kerin T, Ramanathan A, Rivas K, Grepo N, Coetzee GA, Campbell DB. A noncoding RNA antisense to moesin at 5p14.1 in autism. *Science Transl Med* 2012; **4**: 128ra140.
- Sperow M, Berry RB, Bayazitov IT, Zhu G, Baker SJ, Zakharenko SS. Phosphatase and tensin homologue (PTEN) regulates synaptic plasticity independently of its effect on neuronal morphology and migration. *J Physiol* 2012; **590**(Pt 4): 777–792.
- Kwon CH, Luikart BW, Powell CM, Zhou J, Matheny SA, Zhang W *et al*. Pten regulates neuronal arborization and social interaction in mice. *Neuron* 2006; **50**: 377–388.
- Wen Y, Li W, Choudhury GR, He R, Yang T, Liu R *et al*. Astroglial PTEN Loss Disrupts Neuronal Lamination by Dysregulating Radial Glia-guided Neuronal Migration. *Aging Dis* 2013; **4**: 113–126.
- Vargas DL, Nascimbene C, Krishnan C, Zimmerman AW, Pardo CA. Neuroglial activation and neuroinflammation in the brain of patients with autism. *Ann Neurol* 2005; **57**: 67–81.
- Morgan JT, Chana G, Pardo CA, Achim C, Semendeferi K, Buckwalter J *et al*. Microglial activation and increased microglial density observed in the dorsolateral prefrontal cortex in autism. *Biol Psychiatry* 2010; **68**: 368–376.
- Garbett K, Ebert PJ, Mitchell A, Lintas C, Manzi B, Mirnics K *et al*. Immune transcriptome alterations in the temporal cortex of subjects with autism. *Neurobiol Dis* 2008; **30**: 303–311.
- Bourgeron T. A synaptic trek to autism. *Curr Opin Neurobiol* 2009; **19**: 231–234.
- Krumm N, O’Roak BJ, Shendure J, Eichler EE. A *de novo* convergence of autism genetics and molecular neuroscience. *Trends Neurosci* 2014; **37**: 95–105.
- Won H, Mah W, Kim E. Autism spectrum disorder causes, mechanisms, and treatments: focus on neuronal synapses. *Front Mol Neurosci* 2013; **6**: 19.
- Maximo JO, Cadena EJ, Kana RK. The implications of brain connectivity in the neuropsychology of autism. *Neuropsychol Rev* 2014; **24**: 16–31.
- Rudie JD, Shehzad Z, Hernandez LM, Colich NL, Bookheimer SY, Iacoboni M *et al*. Reduced functional integration and segregation of distributed neural systems underlying social and emotional information processing in autism spectrum disorders. *Cerebral Cortex* 2012; **22**: 1025–1037.
- Sgado P, Provenzano G, Dassi E, Adami V, Zunino G, Genovesi S *et al*. Transcriptome profiling in engrailed-2 mutant mice reveals common molecular pathways associated with autism spectrum disorders. *Mol Autism* 2013; **4**: 51.

Supplementary Information accompanies the paper on the Molecular Psychiatry website (<http://www.nature.com/mp>)